Ciência & Engenharia (Science & Engineering Journal) *ISSN 1983-4071*
23 (2): 57 – 66, jul. – dez. 2014

NUMERICAL APPROACH OF THE BOND STRESS BEHAVIOR OF STEEL BARS EMBEDDED IN SELF-COMPACTING CONCRETE (SCC) AND IN ORDINARY CONCRETE IN PULLOUT MODELS

APROXIMAÇÃO NUMÉRICA DO COMPORTAMENTO DA TENSÃO DE ADERÊNCIA DE BARRAS DE AÇO ENVOLVIDAS EM CONCRETO AUTOADENSADO (CAA) E CONCRETO CONVENCIONAL EM MODELOS DE ARRANCAMENTO

Fernando Menezes de Almeida Filho[1], Ana Lúcia Homce de Cresce El Debs[2]
Professor do Departamento de Engenharia Civil (DECiv) da Universidade Federal de São Carlos (UFSCar), São Carlos, SP. E-mail: almeidafilho@ufscar.br
Departamento de Engenharia de Estruturas, Escola de Engenharia de São Carlos (EESC-USP), Universidade de São Paulo (USP), São Carlos, SP. E-mail: analucia@usp.br

ABSTRACT

The main objective of this paper is to analyze by numerical models the bond stress behavior on the steel-concrete interface. Numerical pullout models based on the finite element method were used, considering the nonlinear behavior of the materials. The analyzed parameters were the concrete compressive strength (30 and 60 MPa), the concrete type (self-compacting concrete and ordinary concrete) and the bar diameter (10 and 16 mm). According to the numerical results, a good approach was obtained for the pre-peak branch of the load vs. slip curve for all specimens with different concrete class strength and bar size. The stress distribution presented satisfactory behavior, showing a gradual stress transfer from the beginning to the end of the embedment length.
Keywords: Bond strength; numerical simulation; finite element method; nonlinear behavior; pullout tests.

RESUMO

O principal objetivo deste trabalho é analisar, por meio de modelos numéricos, o comportamento da tensão de aderência da interface aço concreto. Modelos numéricos de arrancamento de barras baseado no método dos elementos finitos foram utilizados, considerando o comportamento não linear dos materiais. Os parâmetros analisados foram a resistência à compressão do concreto (30 e 60 MPa), o tipo de concreto (autoadensável e convencional) e o diâmetro da barra de aço (10 e 16 mm). De acordo com os resultados numéricos, foi obtida uma boa aproximação para o trecho de pré-pico da curva força versus deslizamento para todos os modelos com diferentes classes de concreto e diâmetro da barra de aço. A distribuição de tensões apresentou comportamento satisfatório, mostrando uma gradual transferência de tensão no comprimento de transferência do modelo.
Palavras Chave: resistência de aderência, simulação numérica, método dos elementos finitos, comportamento não linear, ensaios de arrancamento.

1 – INTRODUCTION

Since the development of the usual structures (buildings, bridges and several others) there was a need of optimization of the binary productivity/quality. Or, in other words, maintaining the level of productivity without compromising the level of quality of the structure.

The increase of productivity was always the target of several researches where the studied structures were made of precast concrete, structural masonry or steel. But all these structural systems had a point in common: the productivity associated to the final quality of the structure. In this paper, a reinforced concrete structure is considered.

With the advances obtained in the construction materials and techniques in the last decades, the reinforced concrete is losing some space in the civil construction. This occurs due to several reasons like construction time, curing time, vibration, reinforcement placing and technical staff costs. So, the beginning of self-compacting concrete (SCC) can be associated to a new situation, with durability requirements, reduced cast time and technical staff cost, which brought a new level of competition in relation to the other material applied in structural systems.

The self-compacting concrete is an advanced construction material that can be defined as a mixture that can be cast in any place of the formwork, just through the accommodation of its own weight (Okamura, 1997; Gomes, 2002). Nowadays, the application of self-compacting concrete in structures is target of several researches due to the absence of vibration, which could reveal a weak point to SCC, because of the bond between the steel bar and the adjacent concrete.

The application of SCC is expected to improve the flexural behavior due to its superior filling capability, which could increase the bond between the reinforcement and concrete and, with this capability could indirectly, increase the confinement effect. When SCC is compared to OC (ordinary concrete), for low compressive strength, it possesses a similar bond strength, with some peculiarities (Dehn *et al*., 2000; Holshemacher *et al*., 2002; Almeida Filho *et al*., 2005; Almeida Filho, 2006) and, besides, in places with high reinforcement rate, the fresh properties of

SCC stood out over OC (Chan *et al*., 2003). For high strength concrete, it is expected, as mentioned for low compressive strength, similar results for both concretes, because the high modulus of elasticity. The variation of the modulus of elasticity influences the bond strength, as well as the concrete compressive strength.

The steel-concrete bond is a difficult problem to be represented in the numerical modeling of reinforced concrete elements, and it is not completely understood, because the large number of variables needed to represent the bond phenomena. According to Bangash (1989), the bond stress varies in function of three portions. The first one is the adhesion, which consists of the resistance against shear between concrete and steel; the second is the frictional coefficient, which is a decisive factor for the bond resistance in elements at the ultimate limit state; the last portion is the interaction between the materials (bearing action), which is caused by the deformation of the bars in contact with the concrete.

There are several types of failure associated to the loss of bond between the concrete and the steel bar, and the main ones are pullout failure and splitting failure (Rots, 1989). These failures are strongly influenced by several factors, such as type of reinforcement (bar, tendons and strings), superficial characteristics (flat or rough), bar diameter, presence of confinement reinforcement, distance among the bars, cover, steel bar stress, concrete quality and others.

The numerical simulation requires finite elements that allow steel-concrete relative displacement. The choice of parameters to well represent the contact surface behavior is the main problem to simulate the bond mechanism by means of numerical models. In this case, it is necessary to use contact surface properties that reduce the strain and displacement in the elastic phase, due to the difficulty of such procedure, it is usual to represent the bond behavior in the elastic phase by a very rigid contact surface (Rots, 1989).

In the pullout test of a steel bar from a concrete prism, the failure of the concrete nearly the steel bar surface occurs and the mechanism of pure slip would not be possible (Nielsen, 1998). If a steel bar is placed close to the concrete prism surface, the concrete splitting failure occurs. On the other hand, if no reinforcement is added to the concrete prism, the bond strength depends, almost totally, of the concrete strength. Based on this, several researchers developed constitutive models to evaluate the steel-concrete interface presenting a good agreement (Desir *et at*., 1999; Lee *et al*., 2011).

According to the literature, the studies of the bond strength including self-compacting concrete with steel bars are made in two ways: pullout tests at varying heights in mock-up structural elements and pullout of single bars placed in small prismatic specimens using the Rilem recommendation (Domone, 2007). So, based on this assumption, the use of pullout models to evaluate the bond stress was adopted.

1.1 – Research Significance

Nowadays is more frequent the use of numerical models to represent the behavior of a structure. The recent advances on the computer process and finite element method diffusion brought a new level for the structural analysis. This kind of analysis needs care due to the high sensibility of the numerical model, since a bad use or a bad interpretation of the results could compromise the safety of the structural element.

This concern was the basis of this research, whose objective was to develop a reliable numerical model that could give results in accordance with performed tests. In this case, the considered tests were pullout models cast with self-compacting concrete (SCC) and ordinary concrete (OC), with different concrete strength (30 and 60 MPa) and different steel bar diameter (10 and 16 mm). The absence of data for the evaluation of the bond strength when using self-compacting concrete, the bond behavior on the steel-concrete interface and the need of better representations for the bond stress also gave the motivation for this research.

2 – SUMMARY OF EXPERIMENTAL PROGRAM

The experimental program was part of a research program about the bond behavior on self-compacting concrete. The pullout model geometry (Figure 1) was established by Rilem-CEB-FIP (1973).

Figure 1 – Pullout geometry for 10 mm (a) and for 16 mm (b) steel bar specimens (Almeida Filho, 2006)

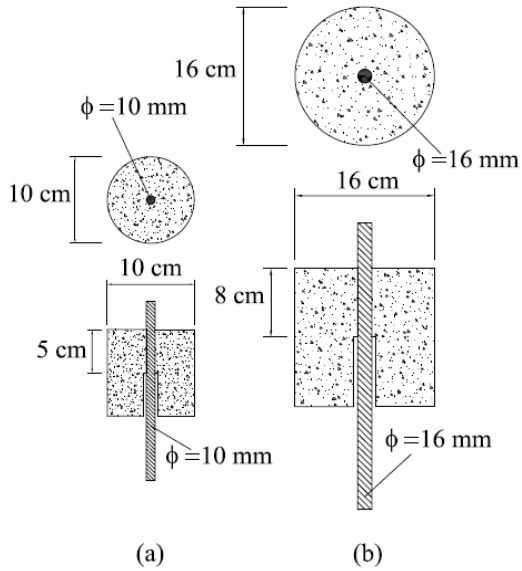

The adopted instrumentation was the same of Rilem recommendation. One LVDT was placed at the top of the steel bar to measure the slip between the steel bar and the concrete cylinder.

The used cement was Ciminas CP-V Ari Plus (Initial High Strength cement). Siliceous sand had density of 2.63 kg/dm^3 and absorption of 4.0% and crushed gravel had density of 2.83 kg/dm^3 and absorption of 1.71%. The

superplasticizer was based on carboxylate with density of 1.1 kg/dm^3 and 20% of solid content. Table 1 shows the materials contents and the results for fresh SCC. Table 2 shows the hardened properties of SCC series and OC series at the time of the tests, at 14 days.

Table 1 – Materials content and fresh properties for SCC series (ALMEIDA FILHO, 2006)

Material	OC1	OC2	SCC1	SCC2
Cement (kg)	365.3	488.3	338.8	365.1
Sand (kg)	883.9	766.6	854.8	815.3
Gravel (kg)	942.3	942.4	919.1	876.7
Water (kg)	260.8	227.0	273.6	146.1
Superplasticizer (%)	---	---	0.4%	0.75%
Filler (kg)	---	---	101.6	146.1
Silica fume (kg)	---	---	---	36.5

Tests	SCC1	SCC2
Slump test		
Slump flow (cm)	67.5	61.0
T_{50} (s)	1.0	1.0
L-Box test		
T_{60} (s)	1.0	1.0
RB	0.95	0.9
V-Funnel		
T_v (s)	1.5	2.0

Table 2 – Hardened properties of the SCC and OC series (ALMEIDA FILHO, 2006).

	OC1	OC2	SCC1	SCC2
f_c (MPa)	32.02	50.20	30.10	53.3
E_c (MPa)	27.24	34308.0	27.87	36686.0
f_{ct} (MPa)	2.182	3.92	2.450	4.99

Where "f_c" corresponds to the concrete compressive strength, "E_c" is the concrete's longitudinal modulus of elasticity and "f_{ct}" is the concrete tensile strength.

The tests were divided according to the concrete type, concrete compressive strength and bar diameter. Table 3 shows the notation for the specimens.

Table 3 – Nomenclature for the pullout specimens (ALMEIDA FILHO, 2006)

Series	Model	Concrete type	f_c	Bar diameter
1	P-SCC-C30-B10	SCC	30 MPa	10 mm
	P-SCC-C30-B16	SCC		16 mm
	P-OC-C30-B10	OC		10 mm
	P-OC-C30-B16	OC		16 mm
2	P-SCC-C60-B10	SCC	60 MPa	10 mm
	P-SCC-C60-B16	SCC		16 mm
	P-OC-C60-B10	OC		10 mm
	P-OC-C60-B16	OC		16 mm

According to Table 3, "P" refers to pullout specimen; "SCC" and "OC" refers to self-compacting concrete and ordinary concrete, respectively; C30 and C60 refers to concrete compressive strength of 30 and 60 MPa; and B10 and B16 refers to the steel bar diameter of 10 and 16 mm, respectively.

The position and the inclination of the bars during the casting have significant behavior in the bond resistance and, like this, the specimens cast in the vertical direction present larger bond resistance, while, the models with horizontal cast present a low bond resistance. In this case, the casting position considered was the first mentioned and a monotonic displacement that changes with the bar diameter; so, for 10 mm steel bar, the displacement rate was 0.01 mm/s and for the 16 mm steel bar, the displacement rate was 0.016 mm/s, until failure.

Figure 2 shows the pullout specimen during tests at the universal test machine, Instron.

Figure 2 – Pullout specimen at test (ALMEIDA FILHO, 2006)

According to the results, the specimens cast with self-compacting concrete and ordinary concrete presented the same behavior. For high strength concrete, the specimens had splitting failure for both bar diameters. However, for normal compressive strength concrete, most of the specimens presented slip failure, except some of the 16 mm steel bar specimens that presented splitting failure, certainly due to the steel bar diameter.

3 – NUMERICAL SIMULATION

A numerical model to predict the behavior of the specimens in pullout tests was developed as part of this study. This model was based on a finite element tool (Ansys®), which admitted nonlinear materials behavior (concrete and steel). Besides, the adopted procedure to evaluate the bond behavior considered contact elements placed on the interface zone between concrete and steel.

According to the used numerical tool, the failure in steel-concrete interface could be attained by combining Coulomb's frictional hypothesis with a bound for the maximum tensile stress, resulting in two different failure modes that could be called sliding failure and separation failure (Nielsen, 1998). The sliding failure, that is the real bond failure, is assumed to occur in a section when the shear stress exceeds the sliding resistance and should be determined by two parameters: the cohesion (c) and the friction coefficient (μ).

3.1 – Description of the model

In previous studies, the variation of the frictional coefficient and the cohesion seemed not to affect the general response of the bond in the contact surface. However, the number of elements in the contact surface, and parameters like FKN (normal contact stiffness factor), FKT (tangent contact stiffness factor), the cohesion (c), the friction coefficient (μ) and IT (iteration number) presented

in the software, affect directly the load *vs*. slip behavior, according to the adopted bond model (De Nardin *et al*., 2005a; De Nardin *et al*., 2005b). Therefore, the value of μ is 0.75, which corresponds to a friction angle of 37º and leads to cohesion of 0.75 kN/cm^2.

The FKN parameter is defined as the normal contact stiffness factor and the usual factor range is 0.01 to 10 (positive or negative). If the value of FKN is low, the contact surface is more flexible and higher values of FKN correspond to a rigid contact surface. The parameter FKT is defined as the tangent contact stiffness factor and has a default value of 1. The range adopted by the software for this parameter is between 0.1 to 1.

The behavior of the contact surfaces presented in the software is described below.

- *Standard*: represents the unilateral contact, *i. e.*, the normal pressure is equal to zero if the separation happens;
- *Rough*: it models the frictional contact without considering the slip;
- *No separation*: the contact surfaces are arrested, but a sliding is possible to occur among the steel and concrete elements, with no separation of the knots;
- *No separation (always)*: there is no separation among contact points that are inside previously to the penetration area established (pinball region). In addition, there is no penetration among the contact elements fixed on the target surface. When there is no penetration, the *No separation* and *No separation (always)* models produce the same results;
- *Bonded*: the contact surface is bonded in all directions;
- *Bonded (always)*: it simulates the separation of the contact points that are initially inside the area of the pre-established penetration (pinball region) or that involve the contact on the target surface along the normal and tangential directions to the contact surface;
- *Bonded (initial contact)*: only the contact elements that are in contact with the target surface at the beginning of the analysis will remain arrested to the objective surface.

For this research, the previous parameters (FKN, FKT, c, μ and IT) were based in previous studies (De Nardin *et al*., 2005a, De Nardin *et al*., 2005b), and the behavior of the contact surface adopted was the "*bonded*".

3.2 – Materials

Compressive strength and elasticity modulus of concrete were obtained by tests in cylindrical specimens (10cm x 20cm). Figure 3 shows the experimental behavior of SCC and OC, for each series, and the steel bar behavior assumed in this numerical study.

There was an absence of the descending branch of the post-peak of its behavior, which could be achieved by using Popovics' formulation (Popovics, 1973), shown below (Eq. 1 to 3).

$$f_c = f_o \cdot \frac{\varepsilon}{\varepsilon_o} \cdot \frac{n}{n - 1 + \left(\varepsilon / \varepsilon_o\right)^n} \qquad \text{Eq. 1}$$

$$n = 0.4 \cdot 10^{-3} \cdot f_o + 1.0 \qquad \text{Eq. 2}$$

$$\varepsilon_o = 2{,}7 \cdot 10^{-4} \cdot \sqrt[4]{f_o} \qquad \text{Eq. 3}$$

This formulation takes into account the variation of the concrete compressive strength in the post-peak branch. According to Popovics' theory, the relation between the initial modulus of elasticity (E_c) and the secant modulus of elasticity (E_{cs}) can vary until 4.0 for normal strength concretes and in 1.3 for high strength concretes. So, the curve made using Popovics' theory was applied in the software for a better accuracy of the result.

Figure 3 – Concrete and steel bar behavior (ALMEIDA FILHO, 2006)

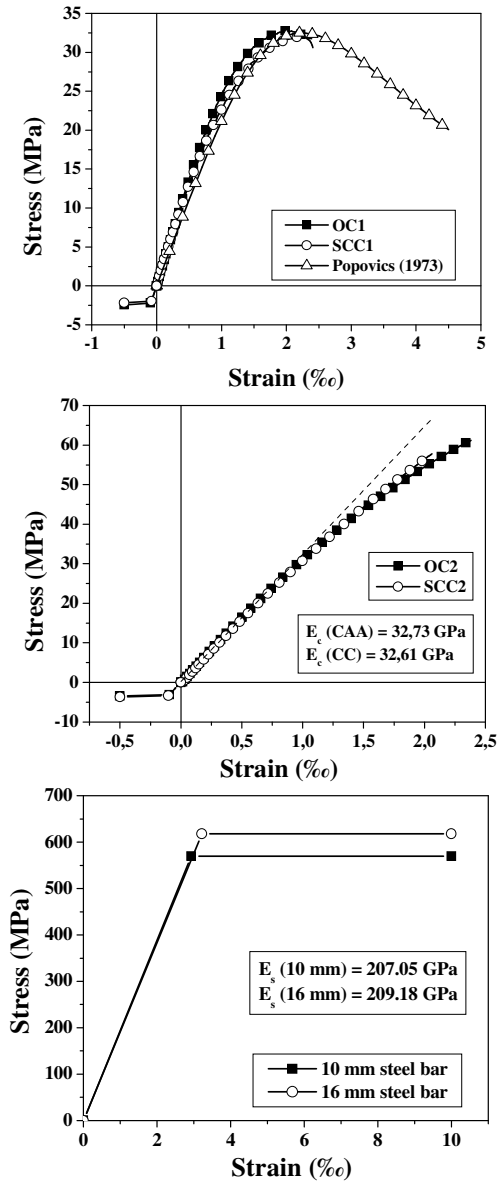

According to Figure 3, for both concrete series, the concrete behavior was almost the same for SCC and for OC. Because of that, the same concrete behavior was adopted for the numerical approach.

3.3 – Geometry and mesh

In Figure 4 is shown the mesh used in the numerical models and, due to the symmetry, a quarter of the pullout model were studied.

Figure 4 – Pullout mesh for 10 mm and 16 mm steel bar

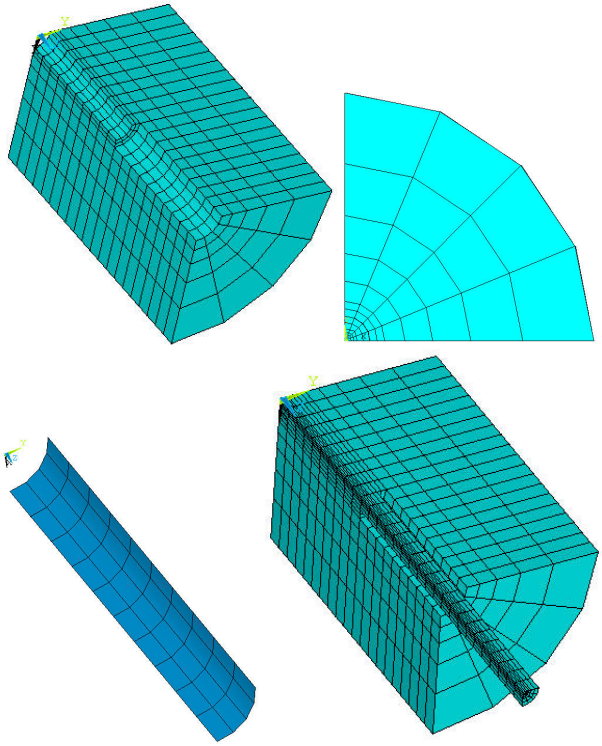

(a) 10mm pullout model mesh discretization

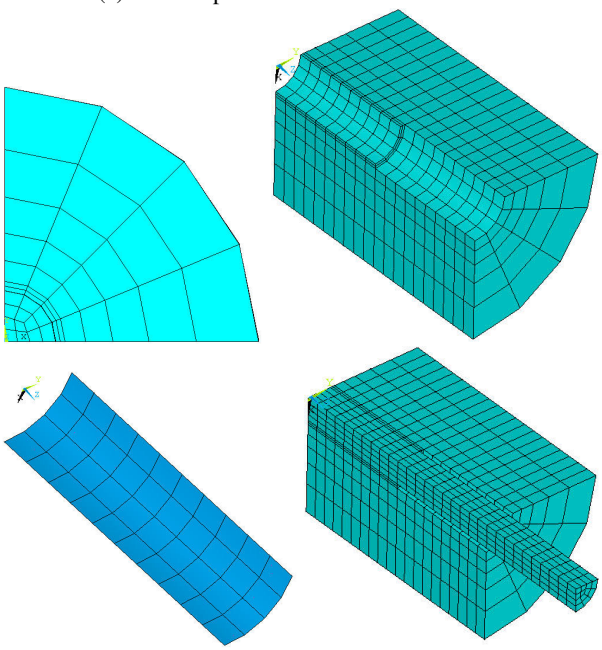

(b) 16mm pullout model mesh discretization

Experimental investigation of the bond stress response was realized using the specimen geometry shown in Figure 1. The specimens for this study consisted of a steel bar with 10 mm and 16 mm of nominal diameter, anchored in 50 mm and 80 mm embedded length in the concrete pullout specimen, respectively.

The finite elements used on the mesh were: for concrete elements, *Solid65*; for steel elements, *Solid45*; for contact surface, *Conta174* and *Targe170* (Ansys®).

In Figure 5 is shown the used constraints for the numerical model, according to the test arrangement.

Figure 5 – Constraints of the numerical model (a) and plain contact surface (b)

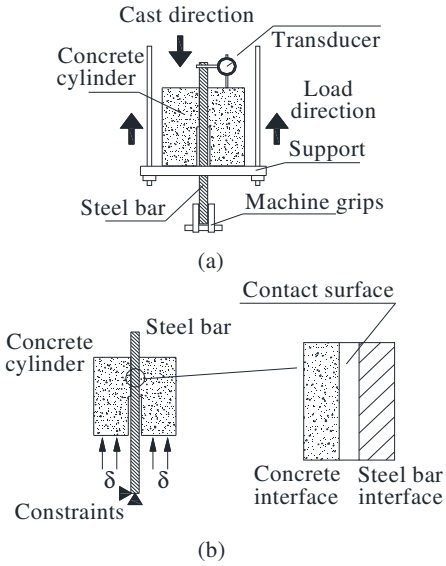

According to Figure 5, the roughness of the steel bar was not considered and a plain contact surface was adopted in the numerical study.

4 – ANALYSIS OF THE RESULTS AND DISCUSSION

This segment presents the analysis between the numerical models and the experimental research made by Almeida Filho (2006).

The parameters used by the software for this research (such as: FKN, FKT, cohesion, friction coefficient and others) were based in De Nardin *et al.* (2005a) and De Nardin *et al.* (2005b).

4.1 – Comparison with experimental results

The comparison was made by using the average result of the pullout tests (5 specimens for series). Figs. 6 and 7 show the comparison between the numerical results and the tests performed.

Figure 6 – Numerical models *vs*. test results for series 1

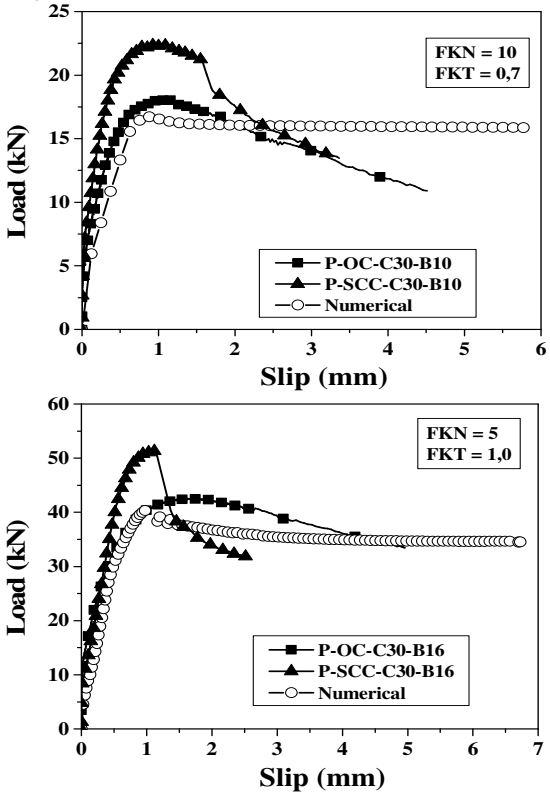

Figure 7 – Numerical models *vs*. test results for series 2

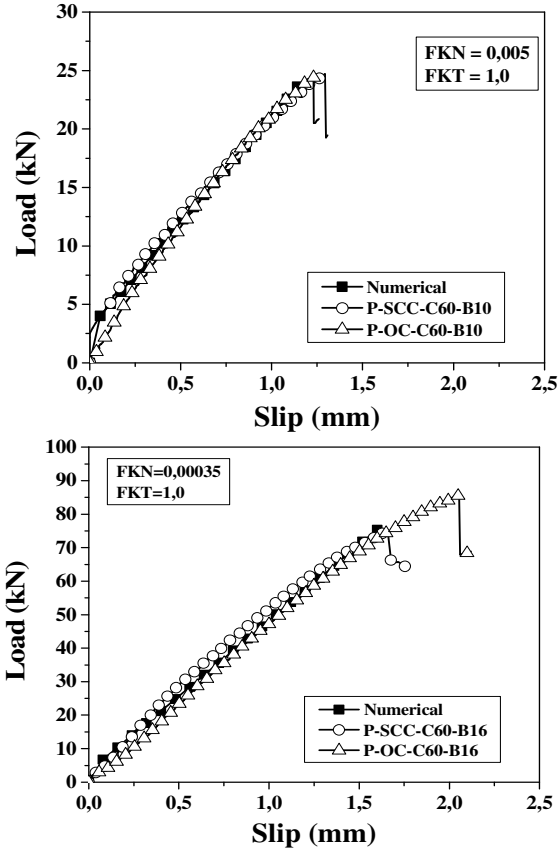

According to Figs. 6 and 7, there was a good approach for the load *vs*. slip behavior of the pullout tests. In addition, the best fit occurred for the models with high strength concrete. The models with normal compressive strength presented a good approach only for the pre-peak branch. For the post-peak branch that did not happen, because this branch is characterized by the gradual loss of bond due of the bearing action that occurs between the steel bar and the existing concrete, which could not be represented by the numerical model.

In Table 4 is shown the comparison of the maximum value for the pullout load and the maximum slip of the numerical models with test results.

Table 4 – Comparison with test results

Series 1					
P-SCC-C30-B10			P-OC-C30-B10		
	Exp.	Num. / λ		Exp.	Num. / λ
P_u (kN)	22,52	16,72 / 1,35	P_u (kN)	18,09	16,72 / 1,08
$s_{u\ (mm)}$	0,96	0,882 / 1,09	$s_{u\ (mm)}$	0,979	0,882 / 1,11
P-SCC -C30-B16			P-OC -C30-B16		
	Exp.	Num. / λ		Exp.	Num. / λ
P_u (kN)	52,01	40,33 / 1,29	P_u (kN)	42,36	40,33 / 1,05
$s_{u\ (mm)}$	1,06	0,98 / 1,08	$s_{u\ (mm)}$	1,64	0,98 / 1,67

Series 2					
P-SCC -C60-B10			P-OC -C60-B10		
	Exp.	Num. / λ		Exp.	Num. / λ
P_u (kN)	24,70	23,61 / 1,046	P_u (kN)	24,44	23,61 / 1,035
$s_{u\ (mm)}$	1,29	1,14 / 1,131	$s_{u\ (mm)}$	1,23	1,14 / 1,079
P-SCC -C60-B16			P-OC -C60-B16		
	Exp.	Num. / λ		Exp.	Num. / λ
P_u (kN)	74,46	75,39 / 0,988	P_u (kN)	85,7	75,39 / 1,137
$s_{u\ (mm)}$	1,65	1,60 / 1,031	$s_{u\ (mm)}$	2,05	1,60 / 1,281

Where, "λ" corresponds to the experimental *vs*. numerical ratio.

According to Table 4, there was good approach of the numerical and experimental results for the load and slip at the test failure. The difference between the results was higher when compared the models with normal compressive strength. This could be explained by the occurrence of slip failure, while the models with high strength concrete failed by the sudden concrete splitting.

4.2 – Analysis of the bond stress

The numerical model had similar parameters, like modulus of elasticity and the applied load, justifying the development of one model for each series. In the contact evaluation, the compared results were obtained from Rilem recommendation, which determinates the bond strength in the pullout test.

The points of measurement were placed at the beginning, at the middle and at the end of the contact zone (Figure 8), to evaluate the bond stress variation on the contact elements and on the concrete elements under the contact surface.

Figure 8 – Measurement points on the contact surface for the pullout numerical models

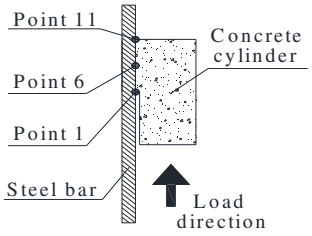

In Figure 9 and 10 are shown the stress variation on the contact zone evaluated by the contact elements and concrete elements for both considered concrete compressive strength. Notice that, for compressive stress the value is positive and for tensile stress the value is negative.

Figure 9 – Stress distribution on the contact surface for the series 1

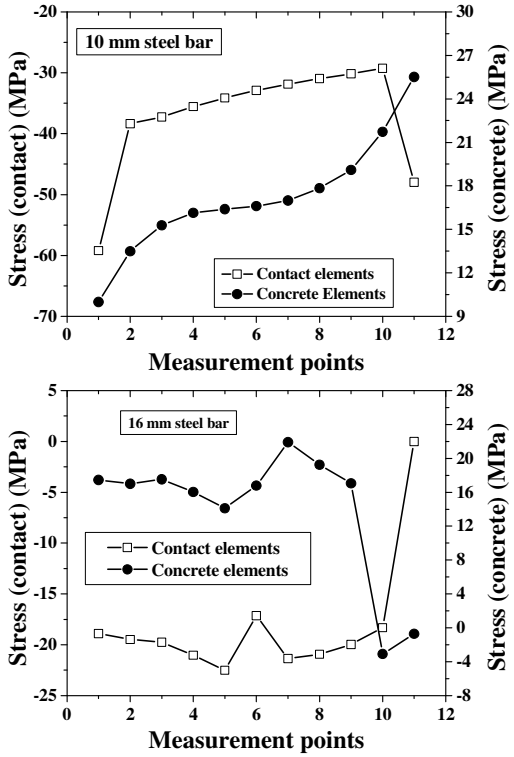

Figure 10 – Stress distribution on the contact surface for the series 2

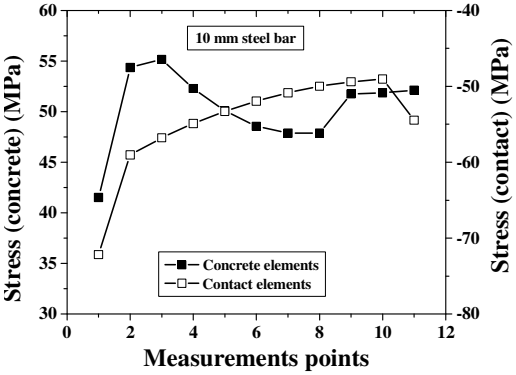

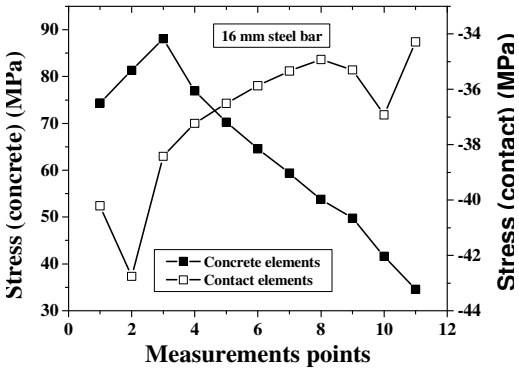

According to these results, it was clear the difference between the stresses from the contact elements and the concrete elements. The stresses determined by the contact elements were tension stresses, while the concrete elements were compression stresses.

In Figs. 11 and 12 are shown the numerical response of the concrete and steel stress distribution (principal stress, σ_3) in the pullout numerical approach. Notice that the stresses presented were displayed as the software configuration, where compression stress assumes negative values and tensile stress assumes positive values.

Figure 11 – Numerical response for the concrete and steel stresses (principal stress, σ_3) for the pullout models from series 1 (stress in kN/cm^2)

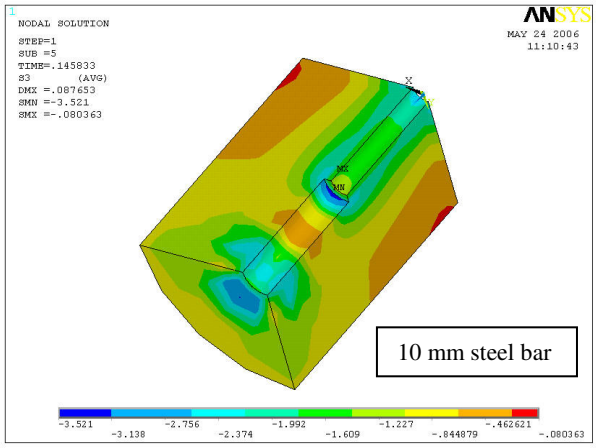

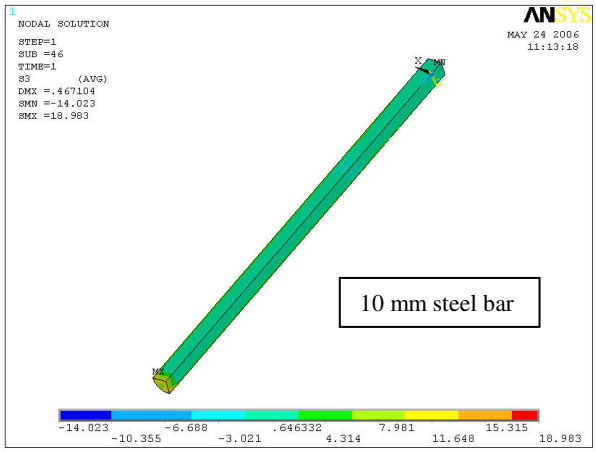

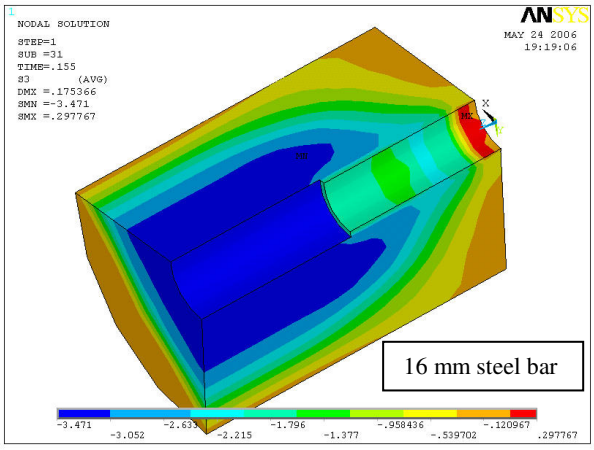

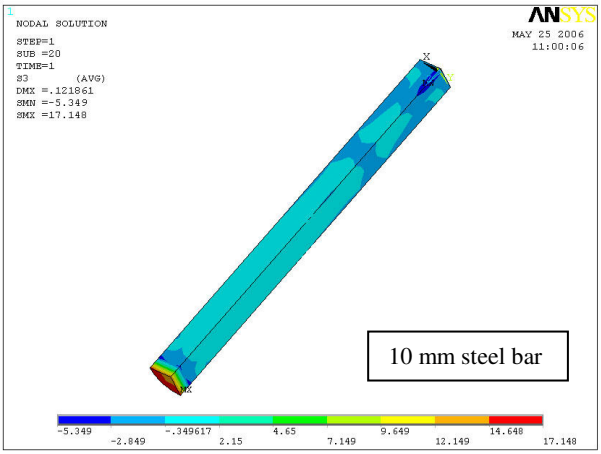

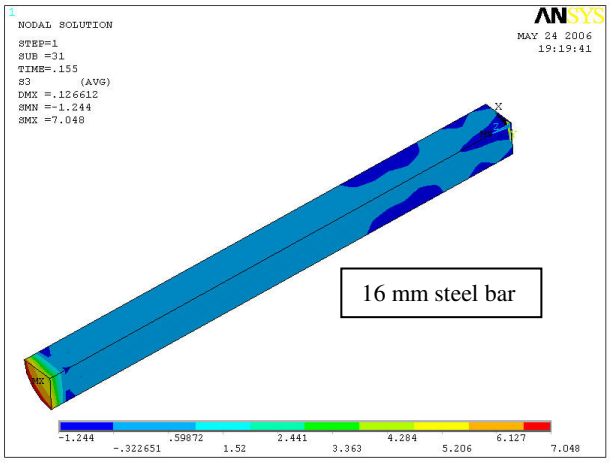

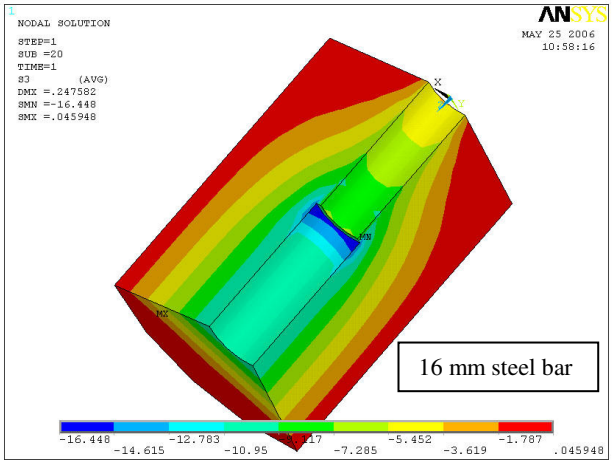

The variation of the stresses for normal compressive strength concrete shows that the maximum tensile strength was not enough to split the concrete cylinder, as expected; however, the stresses for high compressive strength models demonstrated high tensile stress from the edge to the center of the cylinder, with similar values found in the concrete tensile tests.

Figure 12 – Numerical response for the concrete and steel stresses (principal stress, σ_3) for the pullout models from series 2 (stress in kN/cm^2)

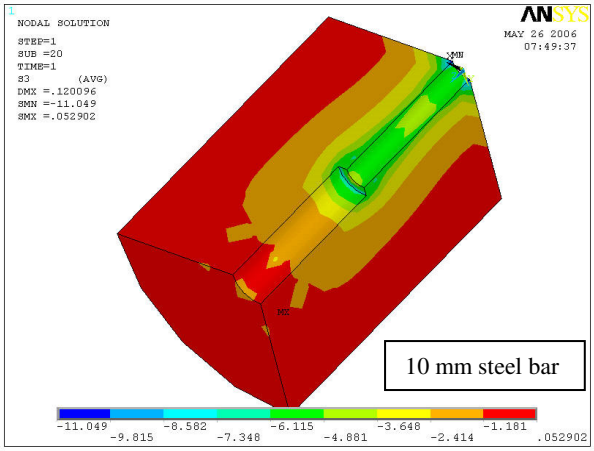

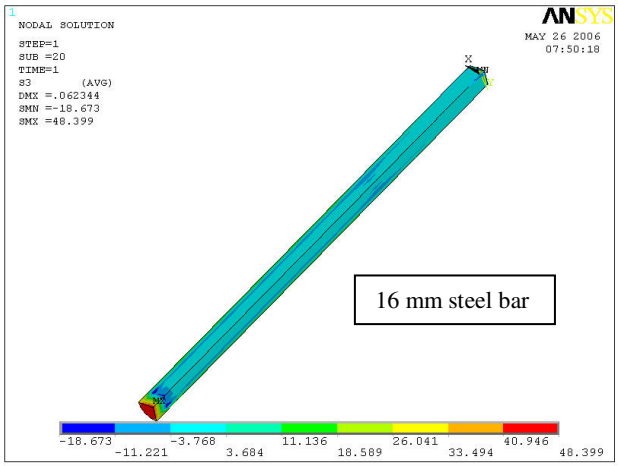

These results demonstrated that the numerical model represented the stress behavior of the test, and in agreement with the expected behavior. Notice that compressive stress is negative and tensile stress is positive, in this case (results from the software).

In Figure 13 and Figure 14 are show the variation of the stress at the contact surface along the test. The measurement points were the same established in Figure 8.

Figure 13 – Stresses on the contact surface from measurement points for series 1

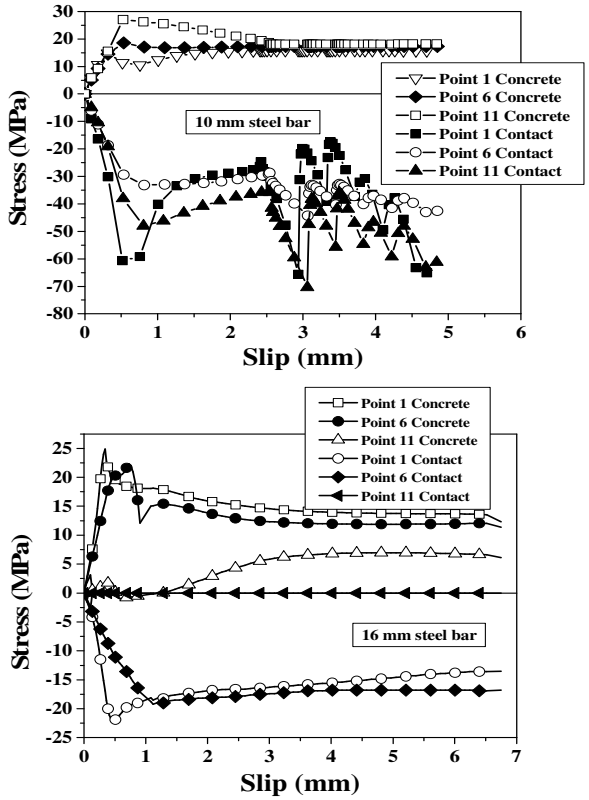

Figure 14 – Stresses on the contact surface from measurement points for Series 2

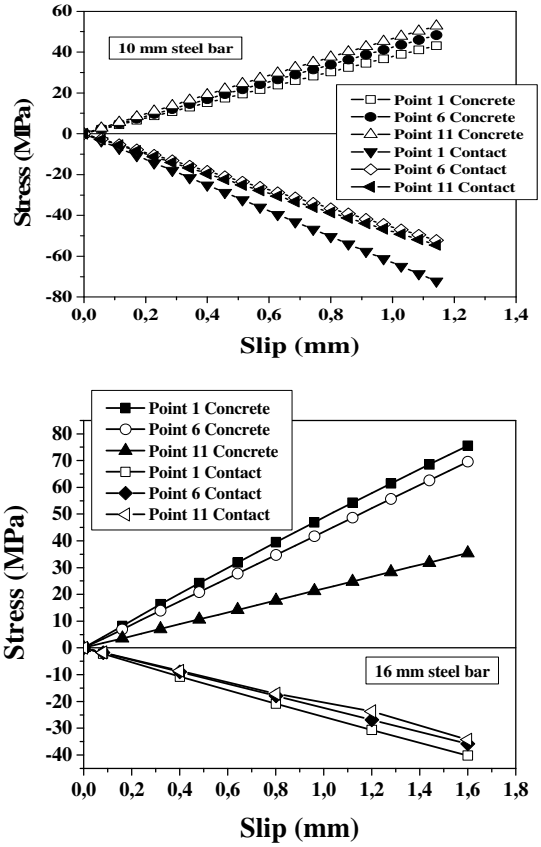

According to the results at Figure 13 and 14, there was a high difference between the behavior of the concrete and contact elements, as mentioned before. The concrete elements presented compression stresses while contact elements presented tensile stresses. For the models from series 1, the model with 10 mm steel bar presented similar behavior for all measurement points, which means that the embedment length was totally used for the slip resistance. The model with 16 mm steel bar presented different values for the point 11, showing that the bond resistance was mobilized mainly until the first measurement points (1 and 6); besides, the point 11 began to be mobilized after a reduction of stresses at points 1 and 6, showing the stress transfer along the embedment length.

For the models from series 2, the behavior was almost linear until the failure of the model. This behavior could be explained by the fragile nature of the test, because the test specimen, as the numerical model, presented small values for the slip. In the same way of the series 1, the models from series 2 with 10 mm steel bar had similar behavior for the measurement points which means that the embedment length was totally mobilized for the slip resistance. The 16 mm steel bar specimen presented similar values for the first measurement points (1 and 6) and the point 11 presented lower values, meaning also the stress transfer on the contact surface.

CONCLUSIONS

The numerical study presented in this paper models the monotonic bond behavior for pullout models cast with self-compacting concrete and ordinary concrete.

Based on the comparison of the numerical pullout model with the experimental test results conducted in previous research, the following conclusions can be made:

1. The load *vs.* slip behavior of the tests, cast with SCC and OC, was always well represented for the pre-peak branch. The post-peak branch from series 1, however, could not be represented by the numerical model due the existing bearing action. This behavior leads to a different numerical approach for each kind of concrete;
2. The values used for FKN and FKT furnish the best approach in this numerical approach, which does not means that this values are the best for another researches. According to the numerical evaluation, the behavior of the materials used in the tests had major significance and this could induce to a variation of the expected result;
3. According to Figure 11, the stress distribution showed that it did not reached the concrete compressive strength, for 10 mm steel bar specimen, but, for 16 mm steel bar specimen, the concrete compressive strength were surpassed resulting in a splitting failure. Figure 12, showed stress distribution compatible with the performed test, once for both steel bar diameters the concrete compressive strength were by far surpassed, reaching values over 80 MPa, resulting in a splitting failure, as occurred in the performed test;
4. The analysis of the development and evolution of the stresses at the contact surface showed that the stresses

at the contact surface, measured in concrete elements and contact elements, gave a good idea of the stress distribution. The evolution of stresses on the contact surface showed the stress transfer from the first measurement points to the last ones (1 to 11);

5. As shown on Figure 6, the numerical approach for SCC pullout specimens were not well represented, due to several factors which could be the different materials used in the concrete at the test and the SCC by itself. More specimens should be tested in order to evaluate if this results repeats denoting a better bond strength for SCC when compared to OC with same compressive strength, in this case, 30 MPa.

Finally, as major conclusion, the load *vs*. slip behavior of the pullout test was satisfactory represented by the numerical model, which means that the contact between steel and concrete, a difficult problem to be solved and correctly evaluated, can be done, giving a good approach of the tests results.

NOTATION

P_u = Failure load, kN;
f_c = Concrete compressive strength, MPa;
s_u = Slip at the failure load, mm;
δ_u = Maximum beam vertical displacement, mm;
λ = Experimental vs. numerical ratio;
f_o = Cylinder concrete compressive strength, MPa;
ε = Strain caused by the f_c concrete stress, ‰;
ε_o = Strain at cylinder concrete failure, ‰;
FKN = Normal contact stiffness factor;
FKT = Tangent contact stiffness factor.

ACKNOWLEDGES

The research group would like to thanks to the CAPES, CNPq and FAPESP for the financial support. Also, to the technical staff at the Structures Laboratory for the support on the development of the pullout tests and to the companies Elkem, Holcim, Grace Brasil and Brasil Minas S/A, for the material donation.

REFERENCES

ANSYS. O**n-line manuals**, Engineering Analysis System, 2011.

ALMEIDA FILHO, F. M. **Contribution to the study of the bond between steel bars and self-compacting concrete**. PhD Dissertation. São Paulo University, São Carlos, Brazil, 2006.

ALMEIDA FILHO, F. M.; DE NARDIN, S.; EL DEBS, A. L. H. C. Evaluation of the bond stress of self-compacting concrete in pullout tests. In: P**roceedings of fourth RILEM international symposium on self-compacting concrete**, Northwestern University, pp.953-958, 2005.

BANGASH, M. Y. H. **Concrete and concrete structures: numerical modeling and applications**. Barking: Elsevier science publishers Ltd., 1989.

CHAN, Y. W.; CHEN, Y. S.; LIU, Y. S. Effect of consolidation on bond of reinforcement in concrete of different workabilities. **ACI Structural Journal,** v. 100, n. 4, p. 294-301, 2003.

DE NARDIN, S.; ALMEIDA FILHO, F. M.; EL DEBS, A. L. H. C. Nonlinear analysis of the bond strength behavior on the steel-concrete interface by numerical models and pullout tests. In: **Proceedings of the ASCE Conference "Structures 2005"**, v. 171, New York, USA, 2005a.

DE NARDIN, S.; ALMEIDA FILHO, F. M.; EL DEBS, A. L. H. C.; EL DEBS, M. K. Steel-concrete interface: influence of contact parameters. In: **Proceedings of the FIB International Conference: "Keep concrete attractive"**, Budapest, Hungary, 6 p., 2005b.

DEHN, F.; HOLSHEMACHER, H.; WEIBE, D. Self-compacting concrete (SCC) time development of the material properties and the bond behavior. In: **LACER**, n. 5, 10 p., 2000.

DÉSIR, J.-M.; ROMDHANE, M. R. B.; ULM, F.-J.; FAIRBAIRN, E. M. R. Steel-concrete interface: revisiting constitutive and numerical modeling. **Computers and Structures**, v. 71, p. 489-503, 1999. http://dx.doi.org/10.1016/S0045-7949(98)00308-3.

DOMONE, P. L. A review of the hardened mechanical properties of self-compacting concrete. **Cement & Concrete Composites**, v. 29, p.1-12, 2007. http://dx.doi.org/10.1016/j.cemconcomp.2006.07.010.

GOMES, P. C. C. **Optimization and characterization of high-strength self-compacting concrete**. PhD thesis. Barcelona, Universitat Politècnica de Catalunya, 2002.

HOLSHEMACHER, K.; DEHN, F.; WEIBE, D. Bond in high-strength concrete – influence of rebar position. In: **6th international symposium on utilization of high strength / high-performance concrete**, Leipzig-Germany, p.289-298, 2002.

LEE, Y.-H.; JOO, Y.T.; LEE, T.; HA, D.-H. Mechanical properties of constitutive parameters in steel-concrete interface. **Engineering Structures**, v. 33, p. 1277-1290, 2011. http://dx.doi.org/10.1016/j.engstruct.2011.01.005.

NIELSEN, M. P. **Limit analysis and concrete plasticity**. CRC Press, 1998.

OKAMURA, H. Self-compacting high-performance concrete. **Concrete International**, v. 19, n. 7, p. 50-54, 1997.

POPOVICS, S. A numerical approach to the complete stress-strain curves for concrete. **Cement and concrete research**, 3 (5), p. 583-599, 1973. http://dx.doi.org/10.1016/0008-8846(73)90096-3.

RILEM-CEB-FIP. Bond test for reinforcing steel: 1-Beam test (7-II-28 D). 2-Pullout test (7-II-128): Tentative recommendations. **Materials and Structures**, v. 6, n. 32, p. 96-105, 1973.

ROTS, J. G. Bond of reinforcement. In: **ELFGREN, L. Fracture mechanics of concrete structures: from theory to applications"**, Report of the Technical Committee 90-FMA Fracture Mechanics to Concrete – Applications, RILEM, Suffolk: St. Edmund Press Ltd, ISBN: 0-412-30680-8, Cap. 12, p. 245-262, 1989.